Feasibility of Laser Scanning to Determine Volumetric Properties of Fine Grained Soils

I. Falcon-Suarez, F. Sanchez-Tembleque, J.M. Rivera-Sar, R. Juncosa-Rivera, J. Delgado-Martin

Abstract. This study analyses the real applicability of laser scanning techniques to determine bulk densities of fine grained soils. The method, fast and accurate, can be employed both in the field and laboratory. The technique was calibrated with benchmarks and then applied to measure volumes of small samples of a specific silty soil of well-known properties (granite sawdust); next transformed into bulk densities from the sample-weights. The results are compared against those obtained from their precursor specimens, made using the Standard Proctor test. Before calculating soil sample volumes, optimum conditions for data acquisition, exportation and post-processing were assessed. The laser scanning provides highly consistent results when compared with those obtained from Standard Proctor compaction tests. However, the study shows a limiting value of moisture content below which the laser scan provides inaccurate results. Likely, this limit varies from soil to soil and therefore the technique must be calibrated before being used to determine bulk densities and derived volumetric properties (*i.e.*, porosity or void ratio). Accordingly, this work presents a helpful procedure to evaluate the applicability of the laser scanning based on the detection of the limiting water content, which considers as well anomalies derived from compositional heterogeneities or external electromagnetic interferences.

Keywords: laser scanning, standard proctor test, bulk density, granite fines.

1. Introduction

The degree of compaction is key parameter on geotechnical works since the permeability and coefficient of consolidation decrease with the reduction of void ratio for a given soil. Hence, when considering final applications in large scale contexts, the materials are subjected to adequate compaction procedures. The aim is to achieve the optimal conditions of the soil, in correspondence to those identified in the laboratory by the use of either standards or widely accepted tests - normal and modified Proctor tests (ASTM D698-07; ASTM D1557-09); moisture condition value (MTV) test (Murray *et al.*, 1992).

In soils, the degree of compaction is defined by two parameters: dry density and water content. Far from trivial, the determination of index volumetric properties (bulk density, void ratio, porosity) is addressed with special techniques which aim at characterizing bulk density and derived properties both in the field and in the laboratory. Such techniques show advantages but also inconveniences (Grossman & Reinsch 2002): the radiation method (Al-Raoush & Papadopoulos 2010; Timm *et al.*, 2005) requires special safety procedures to ensure that undue exposure to gamma radiation is avoided; the soil clod and volume excavation methods (sand or water replacement) are cumbersome; the core-cutter method, although straightforward, depends upon the skills of the operator and on the suitability of the equipment and facilities (*i.e.*, possible over-compaction effects due to the penetration of the corer); other emergent techniques include the use of Thermo-TDR (Liu *et al.*, 2014) or FDR sensors (Al-Asadi & Mouazen 2014) for calculating soil bulk densities indirectly from the dielectric response of the soil, although the results are mainly representative of the piece of soil located in the needle spacing of the probe.

Sander *et al.* (2007) and Rossi *et al.* (2008) propose a method to determine bulk density of grained soils based on the application of high precision laser scanning techniques to irregularly shaped soil samples. Their results show excellent agreement to other conventional methods. Furthermore, the technique is clean and easily reproducible. The main inconvenience is that the method limits its applicability at the laboratory scale, although this is only dependent on the laser scan model used.

So far, the laser scanning technique has been assessed on soil samples at controlled conditions of water content and compaction. In this contribution, the influence of moisture content and degree of compaction on the results obtained is

Ismael Falcon-Suarez, PhD, Postdoc Researcher, Marine Geosciences, National Oceanography Centre, University of Southampton Waterfront Campus, SO143ZH, Southampton, United Kindom. e-mail: isfalc@noc.ac.uk.
Felix Sanchez-Tembleque, PhD, Professor Assistant, Departament of Mathematics and Representation Methods, Civil Engineering School, University of A Coruna, Campus Elvina, A Coruna, Spain, and CITEEC, University of A Coruna, Campus Elvina, A Coruna, Spain. e-mail: fsanchez@udc.es
Jose Maria Rivera-Sar, MSc, Department of Construction Technology, Civil Engineering School, University of A Coruna, Campus Elvina s/n, 15071, A Coruna, Spain. e-mail: riverasar@gmail.com.
Ricardo Juncosa-Rivera, PhD, Associate Professor, Department of Construction Technology, Civil Engineering School, University of A Coruna, Campus Elvina, A Coruna, Spain. e-mail: rjuncosa@udc.es.
Jordi Delgado-Martin, Professor, Associate Professor, Department of Construction Technology, Civil Engineering School, University of A Coruna, Campus Elvina, A Coruna, Spain. e-mail: jdelgado@udc.es.
Submitted on March 19, 2014; Final Acceptance on February 6, 2015; Discussion open until December 31, 2015.

evaluated when applying the laser scanning technique for determining bulk densities on fines. The soil used consisted of two varieties of a particular grain fined material of well-known properties (*i.e.*, granite sawdust or granite fines). Mixing soil and water at different ratios, a trial of Standard Proctor tests were performed towards achieving homogenous soil specimens (*i.e.*, well-distributed moisture and degree of compaction); next, from each specimen a smaller sample was cut to scan. The study assesses the influence of soil composition and moisture on the quality of results, but also how the laser scanning signal could be affected by the presence of metallic particles within the soil matrix.

2. Materials and Methods

The so called granite sawdust or granite fines is the fine grained material used in this study. Granite fines cover the particular waste generated by the dimension stone industry of Galicia (Spain). There, the rock blocks quarried or arrived from other countries, are typically transported to the workshops where they are elaborated before being sold. The elaboration processes involve mechanical activities of abrasive nature (cutting and polishing). Consequently, a wide amount of dusty material is produced every year (*i.e.* granite fines).

After an initial geotechnical characterization, different research lines derived toward applying granite fines in real civil engineering contexts. A comprehensive characterization of the granite fines is given in Delgado *et al.* (2006) and Barrientos *et al.* (2010), while a number of its different applications are described in Vázquez *et al.* (2007), Navarro *et al.* (2008) and Falcon (2011). As a result, granite fines has become into a material of well-known properties, which can be used as reference soil. Accordingly, it is worth mentioning the recent work presented by Falcon *et al.* (2014) in which the granite saw dust is used to test a new technique to determine the permeability of unsaturated soils.

In short, granite fines is a silty material (10-15% clay; 70-75% silt; 10-15% fine sand) with low plasticity (class ML in the USCS classification scheme) and specific surface (6 to 10 $m^2\ g^{-1}$). The mineralogy, consistently with its origin, is dominated by silicates (quartz, microcline, plagioclase, biotite, muscovite, chlorite) plus other accessory minerals associated with the manufacturing processes (calcite and steel grit; 3 and up to 16 wt%, respectively). Compositionally, two main types of granite fines (GF) can be distinguished according to the practices applied on the workshop of provenance: steel grit-bearing (GF1) or not (GF2). The relatively high content of steel grit particles raises the solid density of the GF1 to an average value of ~3190 kg m^{-3}, while GF2 present a common granite value of ~2600 kg m^{-3}.

2.1. Sample performance

To test the laser scanning technique described next, compacted specimens of granite fines plus water at different soil/water ratios were performed applying standard effort energy as described in the ASTM D698-07e1 reference standard (*i.e.*, Standard Proctor test), using a stiff steel mould of known capacity (see Fig. 1). Since granite fines originally present water content ~38% (*i.e.*, when generated in the elaboration workshops), as a first step, the material was oven-dried. Next, granite fines were dampened at different soil/water ratios to obtain specimens which cover the whole range of moistures.

Granite fines and water were mixed to perform 32 Standard Proctor tests (19 of GF1 and 13 of GF2), according to the ASTM D698-07. Bulk and dry densities were computed after the careful differential weighting of the empty/filled mould and the precise knowledge of the moisture content through oven-drying at 105 °C (ASTM D2216-10el). The accuracy of the density determination according to the equipment used (*i.e.*, commercial weight balance and digital Vernier caliper) was ~1%.

Each Proctor specimen (circa 1 dm^3) was halved: one half for laser scanning; the other for determining moisture content. The halves for scanning were carved with the aid of a sharp blade (a wire sculpting tool would also perform well). The flat surface at both ends of the specimen, resulting from the compaction procedure, was used to make hilly polyhedrons with flat base (see Fig. 1 and Fig. 2). This shape makes easier the calculation of sample volumes by integrating the upper surface over a constant base level. Prior to scanning, the sample is weighted directly after being cut in order to avoid moisture changes because exposure to the atmospheric conditions in the laboratory. Finally, dry density is computed with the dry-weight and the calculated volume. Keeping bearing the different measurement techniques employed in the density determination with a laser scanner (*i.e.* volume uncertainty and weighting error), the overall relative error of this technique has been evaluated in less than 0.1%.

Figure 1 - Typical elements of the sample performance: (1) Standard Proctor test mould; (2) Standard Proctor test specimen; (3) small samples, cut from the specimen; (4) the cut tool.

Figure 2 - Carved samples of granite saw dust with (GF1) and without (GF2) steel grit particles.

2.2. The 3D scanning technique

The Polhemus FastSCANTM system is a lightweight, portable line scanner that captures accurate 3D contours of opaque subjects using a built-in diode laser (λ = 670 nm; power = 1 mW) and two miniature digital cameras. It is worth mentioning that the equipment consists of class 2 laser product which means it is safe because the blink reflex will limit the exposure to no more than 0.25 s, as is specified by the IEC 60825-1 standard. The laser and the digital cameras are mounted in a special bracket (transmitter) that holds three orthogonal magnetic coils that pulse an electromagnetic field that allows its accurate tracking with respect to a receiver reference table. FastSCANTM projects a fan of laser light on the object of interest while the cameras view the laser to record cross-sectional depth profiles and render a real-time 3D reconstruction of the object.

The system uses a constant line scanning rate of 50 Hz while the resolution along the laser line is related to the object-scanner distance (0.1 to 0.5 mm at 200 mm distance). The resolution between scanned lines depends on the speed of the sweep of the laser system over the surface of the object while being scanned (1 mm at 50 mm s^{-1}). In this context, Rousseau *et al.* (2012) studied the problems that can be found during scanning mineral surfaces at very high resolutions, pointed out that scanning speed is a crucial aspect to keep bearing. They argued that the faster the speed, the more likely the scanning process remain incomplete; unlike, if it is too low, although the number of measured points makes the data processing complicated, it leads to a better mapping (*i.e.*, resolution is greatly improved when sweeping is slow). Accordingly, the distance to the object was set in 200-250 mm, and 10-20 mm s^{-1} for scanning rate. Fig. 3 shows a typical scanning procedure over a sample of granite fines.

The 3D data generated in the scanning process is stored in a computer: scatter plots or a mesh of triangular facets suitable for exporting to a number of file formats used for late post-processing (González *et al.*, 2007). In the present case, post-processing focused on the quantification of volumes was carried out with Surfer® 10.4 (Golden Software, Inc).

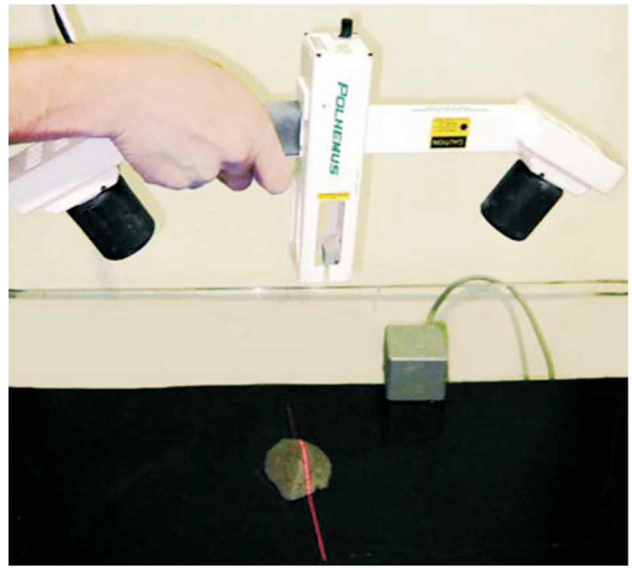

Figure 3 - Typical laser scanning procedure over a sample of granite fines.

2.3. Instrument calibration

Nixon *et al.* (1998) cautioned on the negative influence of local electromagnetic fields and their potential effect in distorting the tracking signal. To evaluate this effect within the workspace, a calibration process was carried out using two benchmarks consisting of polyhedrons made of plastic polymer and machined in a workshop with a precision lathe. The polyhedrons presented pyramidal shapes (*i.e.*, P1 and P2; see Fig. 4), differing in the finish: P1 is a common pyramid, while P2 makes a bent in the middle, resulting in a double-pyramid shape. The corresponding volumes (167.4 and 209.7 cm^3 for P1 and P2, respectively) were computed from fundamental geometric relationships, according to the nominal dimensions reported by the fabricant and verified with a digital Vernier caliper.

2.4. Optimum conditions for data acquisition

Surfer® implements a wide number of interpolation algorithms able to generate regular grids from unevenly spaced scatter data; next, the software allows the user to

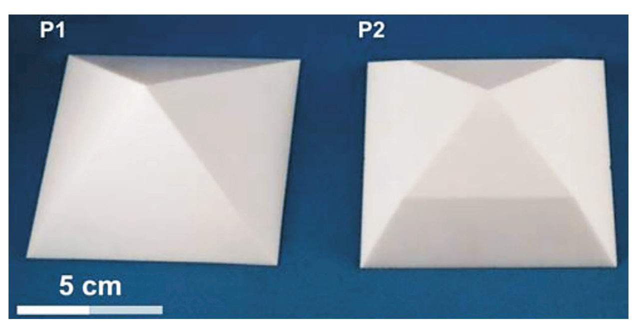

Figure 4 - Polyhedrons of reference employed in the calibration of the 3D laser scanner.

compute the surface-constrained volume from the regular grid. The accuracy of the volume calculation depends on the density of the grid and the method used for interpolation. The first grid is interpolated from the raw data recorded with the laser scanner. So that, it is expected to improve the accuracy of results with a regular grid of points equally distributed (*i.e.*, interpolating points between original raw data).

In this study, it has been considered the performance of twelve gridding algorithms in Surfer® to address with the study of the optimum conditions for post-processing: inverse-distance-to-a-power (IDP); kriging (KG); minimum curvature (MC); modified Shepard's method (MSM); natural neighbour (NN); nearest neighbour (NeN); polynomial regression (PR); radial basis function (RBF); triangulation with linear interpolation (TLI); moving average (MA); data metrics (DM); and local polynomial (LP). From each one of them it is obtained an inferred volume (V_{inf}) that, for the purpose of calibration, can be compared with theoretic volume (V_{the}). The relative volume difference (ΔV_{rel}, in %) can be computed from the following equation:

$$\Delta V_{rel} = \frac{|V_{inf} - V_{the}|}{V_{inf}} \times 100 \tag{1}$$

3. Results and Discussion

3.1. Optimum tuning settings and gridding

Fig. 5 to Fig. 8 illustrates the results of the settings and gridding calibration process. The two benchmark pyramidal shapes (P1 and P2) are scanned using four smoothness/resolution pair (Sm/Res in mm/mm) corresponding with each figure (*i.e.*, Sm/Res = 0.5/0.5, Fig. 5; Sm/Res = 0.5/1, Fig. 6; Sm/Res = 1/1, Fig. 7; Sm/Res = 1/1.5, Fig. 8). Then, the raw data file is converted into volume by the twelve gridding algorithms of Surfer described in the previous section, independently for both P1 and P2, and the results expressed in terms of relative volume difference against the theoretical volume (Eq. 1).

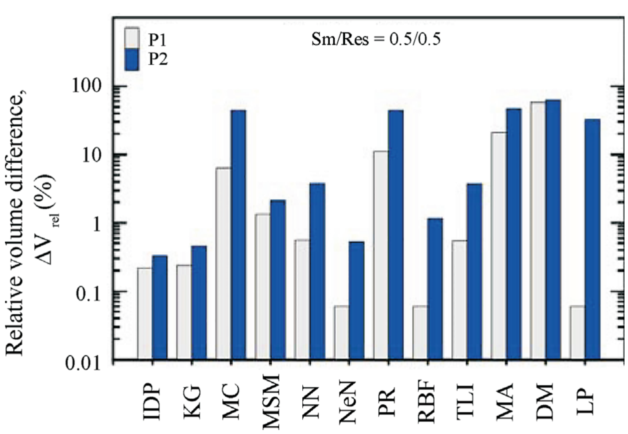

Figure 5 - Twelve methods gridding at Sm/Res = 0.5/0.5.

The results shown in Fig. 5 to Fig. 8 lead to point out some interesting observations. First, according to the experimental settings (*i.e.*, distance to the object and scanning rate), ΔV_{rel} presents minimums when the raw data is exported with a smoothing factor of 0.5 mm; however, resolution ranges between 0.5 and 1 mm without significant

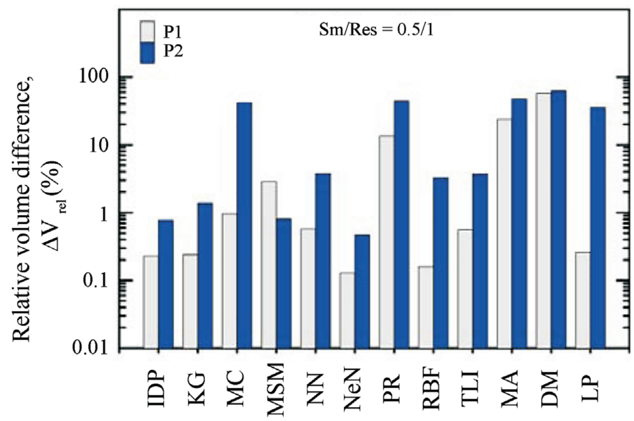

Figure 6 - Twelve methods gridding at Sm/Res = 0.5/1.

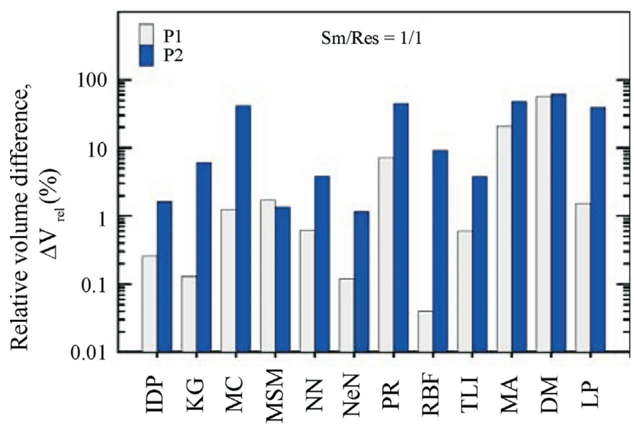

Figure 7 - Twelve methods gridding at Sm/Res = 1/1.

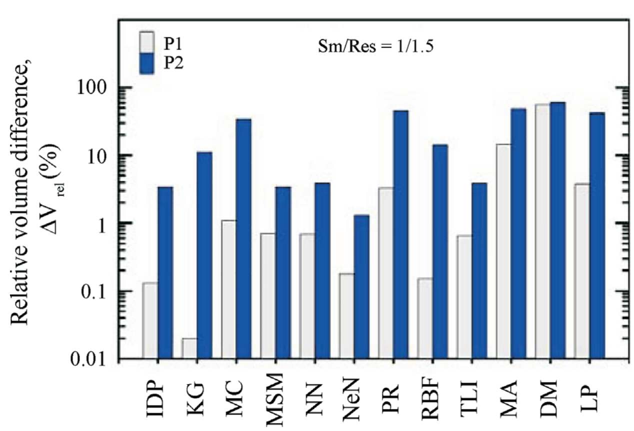

Figure 8 - Twelve methods gridding at Sm/Res = 1/1.5.

differences. Second, some methods show great differences between P1 and P2, which means that they clearly depend on the shape of the scanned surface, being P2 the most affected. Third, it can be observed that calculated volumes greatly vary depending on the considered gridding algorithm. Furthermore, in connection with the work of Yilmaz (2007), the best results are given by the minimum curvature radial basis function, kriging, natural neighbour, triangulation with linear interpolation, nearest neighbour and inverse distance to a power; while the poorest are obtained by MC, PR, DM, and MA.

Among best set of methods mentioned above, the inverse-distance-to-a-power (IDP) and nearest neighbour (NeN) interpolation lead to minima ΔV_{rel}. Although either IDP or NeN is expected to provide good results, this study has been conducted applying the former and using a par-setting smoothing/resolution of 0.5/0.5 mm to the raw data.

3.2. Scanning technique on granite fines

From the Standard Proctor bulk specimens it is obtained a value of dry density and water content. This pair is adopted as the reference values for the sample that is posteriorly cut and scanned from the specimen. The approximation shown in Eq. 1 can be modified in order to study the relative difference of dry densities ($\Delta\rho_{d,REL}$) between the Standard Proctor specimen ($\rho_{d,ASTM}$) and that of the sample cut and scanned from the specimen ($\rho_{d,LS}$). Thus, the expression becomes into the following:

$$\Delta\rho_{d,REL} = \frac{|\rho_{d,ASTM} - \rho_{d,LS}|}{\rho_{d,ASTM}} \times 100 \quad (2)$$

Figure 9 compares the relative dry density difference and the corresponding water content (constant for a given Standard Proctor specimen). It shows that the higher the water content, the smaller the relative dry density difference. A closer look reveals that, when the water content drops below 20%, $\Delta\rho_{d,REL}$ sharply increases (up to 40% if moisture ranges 5 to 10%; see the grey area on Fig. 9). For water contents higher than 20%, $\Delta\rho_{d,REL}$ reduces to a range between 0.1 to 2%.

Figure 10 illustrates the same fact by the direct comparison of dry densities. Those samples of water content higher than 20% show good correlation. Moreover, $\rho_{d,LS}$ is lower than $\rho_{d,ASTM}$ when the water content is below 20%. Figure 10 is therefore suggesting that the consistence of the Proctor specimen decreases after being extracted from the mould and shaped to scanning when the water content is lower than 20%. It can be interpreted as a bulking effect connected with the reduced adhesion of small solid particles, when capillary bridges become less effective and, consequently, the sample losses cohesiveness (Paajanen *et al.*, 2006; Zhang *et al.*, 2008).

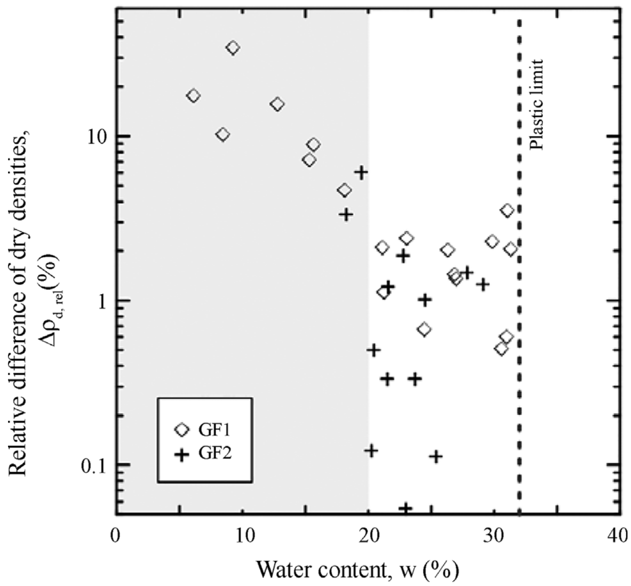

Figure 9 - Dry density difference ($\Delta\rho_{d,REL}$, in %) *vs.* water content, from granite fines samples with (GF1) and without (GF2) steel grit particles.

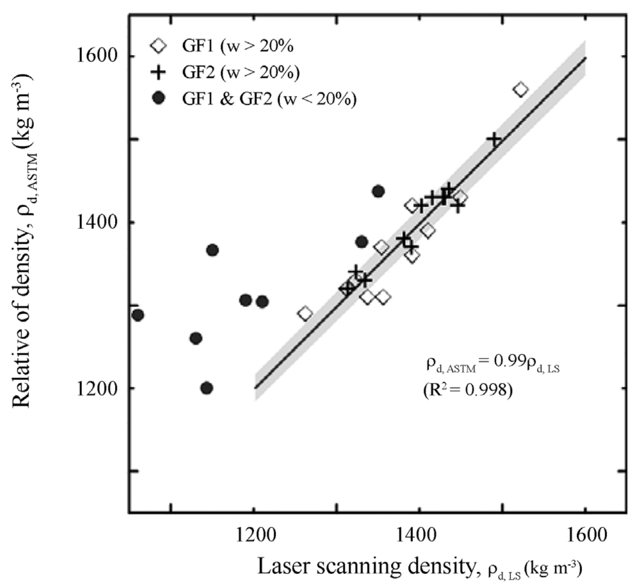

Figure 10 - Dry density from scanner ($\rho_{d,LS}$) *vs.* those from the Standard Proctor tests ($\rho_{d,ASTM}$), of granite saw dust samples with (GF1) and without (GF2) steel grit. Solid line is a linear fit (95% confidence, grey band).

3.3. Heterogeneities in the soil matrix

GF1 samples display slightly higher dispersion than GF2, according to the relative density differences observed (Fig. 9). This effect is likely related to the presence (GF1) or absence (GF2) of steel grit particles in the sample. The proportion of heavy fine grained steel particles within the granite fines matrix is random, independently of the scale. Moreover, steel grit preferentially forms local aggregates within the granite fines matrix (Vazquez *et al.*, 2007; Barrientos *et al.*, 2010; Falcon, 2011).

The effect of heterogeneous steel grit distribution on the dry density is analysed through Fig. 11, that shows the Proctor test results in a common soil-compaction graph (*i.e.*, dry density *vs.* water content), on which polynomial fits for both types of granite fines are also provided. The zero air voids (ZAV, *i.e.*, the theoretic saturation line) differs from GF1 to GF2. However, Proctor tests result on similar values either the type of granite fines. It can be interpreted that, although a low percentage of steel substantially increases the mean value of the density of solid particles (used to theoretically calculate the ZAV of a given soil), the effect on the final bulk weight is scale-dependent: the smaller the sample size, the more sensitive it is to lead unexpected high weights as a result of local high steel content and, consequently, anomalous high dry densities.

The presence of steel grit appears to be a rather specific issue concerning the granite fines that has been addressed from the viewpoint of the increase of the samples weights. However, there is another effect to keep bearing: steel grit may carry to anomalies in the quality of the signal. The presence of magnetic steel grit particles raises also the question of whether they can distort or not the electromagnetic field used to track the position of the scanned surface. To this respect, Nixon *et al.* (1998) indicate that ferromagnetic materials can induce variations in the scanned position but this effect reduces with the size of the ferromagnetic particle. Keeping bearing the average granulometry of GF1 (~20 μm), the results illustrated by these authors demonstrate that the distortion effect associated to the presence of steel grit particles is negligible when compared with the resolution provided by the apparatus. Therefore, the increased dispersion observed in the GF1 samples is attributable to local heterogeneities in the steel grit distribution rather than inferred instrumental errors.

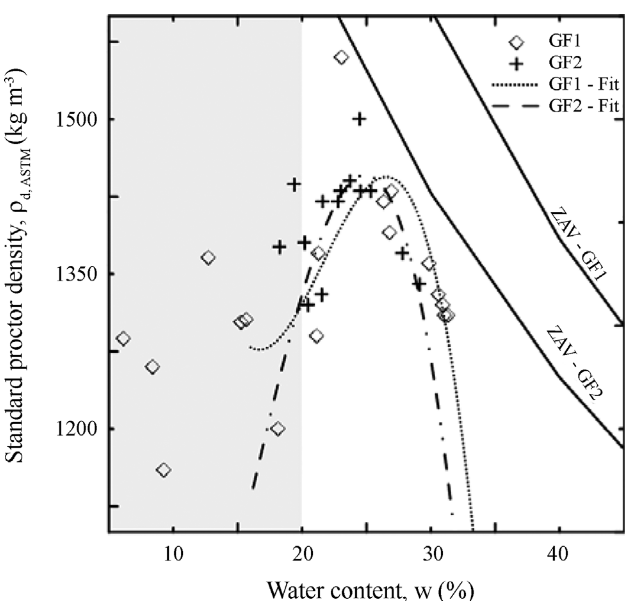

Figure 11 - Results of Standard Proctor tests performed with granite fines with (GF1) and without (GF2) steel grit. Dashed curves represent best third-degree polynomial fits; ZAV, is the Zero Air Voids line (saturation line).

3.4. Applicability of the laser scanning technique on real contexts

Although other authors present lower resolutions of work (Sander *et al.*, 2007; Rossi *et al.*, 2008), our results show how resolutions of 0.5 mm improve the accuracy of density determinations (0.1%) when comparing with the Standard Proctor procedure (1%) worldwide used to specify compaction requirements for roadway construction. Furthermore, the methodology applied in this study (including the sharping, pre-process, and the scanning), last no more than 2 min per sample, which significantly differs from the 40 min proposed by Rossi *et al.* (2008) whom use a similar technique at higher resolutions of about 0.13 mm. In addition, Rousseau *et al.* (2012) argued that scanning under very high resolutions may lead to record some atypical points associated either with the orientation of some minerals or their own optical properties.

In relation with the performance of the laser scanning technique it has been identified a strong dependence respect to the water content of the soil: those samples with lower water content give higher deviations. Such a behaviour, that it is likely to vary from soil to soil, appears to be related with a bulking effect associated to the reduction in the adhesion of solid particles when the attraction force of capillary water becomes small. Although this effect could be reduced by increasing the size of the samples, the uncertainty of the measurement could lead to inaccurate results. Rather, more appropriated is to calibrate the laser scanning technique for a given soil to identify the water content that represents the limit of applicability, and any other anomalies that might affect the measurements.

4. Conclusions

This study has assessed the feasibility of the laser scanning technique to measure bulk densities of fine grained soils. The technique has been studied with samples of granite sawdust as reference material because of their well-known properties. This work presents a singular methodology to address the determination of bulk density of soils which covers, first, the cutting and shaping of granite fines samples performed using the Standard Proctor test procedure and, next, the 3D scanning of the samples and the integration of the scanned surfaces into volumes.

The laser scanning technique provides a fast and accurate method to monitor bulk density but also derived volumetric properties of soils, plausible to be used either in the laboratory or in the field. However, a limiting water content below which the technique is unappropriated was identified. This limit factor is likely related with the cohesiveness of the granite sawdust below moistures of ~20%. This value is specific of the tested material, which suggests the technique must be calibrated from soil to soil. To this respect, the use of Standard Proctor specimens as benchmarks ensures homogenized soil samples to calibration while covering the entire range of moisture content. The simplicity and fastness of the methodology applied in this work (reshaping samples from Proctor benchmarks) make it suitable to address with the calibration of the laser scanning on fine grained soils.

Acknowledgments

Funds for this work have been provided by the Ministry of Science and Innovation (BIA2005-07916-C02-01), Xunta de Galicia (10REM003CT & 10MDS007CT) and the European Regional Development Funds 2007/2013.

References

Al-Raoush, R. & Papadopoulos, A. (2010). Representative elementary volume analysis of porous media using X-Ray computed tomography. Powder Technology, 200(1-2):69-77.

Al-Asadi R.A. & Mouazen A.M. (2014). Combining frequency domain reflectometry and visible and near infrared spectroscopy for assessment of soil bulk density. Soil and Tillage Research, 135:60-70.

ASTM (2007). Standard Test Methods for Laboratory Compaction Characteristics of Soil Using Standard Effort (12 400 ft-lbf/ft (600 kN-m/m)) - D698-07. ASTM International, West Conshohocken, Pennsylvania, USA, 13 p.

ASTM (2009). Standard Test Methods for Laboratory Compaction Characteristics of Soil Using Modified Effort (56,000 ft-lbf/ft3 (2,700 kN-m/m3)) - D1557. ASTM International, West Conshohocken, Pennsylvania, USA, 10 p.

ASTM (2010). Standard Test Methods for Laboratory Determination of Water (Moisture) Content of Soil and Rock by Mass - D22160-10. ASTM International, West Conshohocken, Pennsylvania, USA, 7 p.

Barrientos, V.; Delgado, J.; Navarro, V.; Juncosa, R.; Falcon, I. & Vazquez, A. (2010). Characterization and geochemical-geotechnical properties of granite sawdust produced by the dimension stone industry of O Porrino (Pontevedra, Spain), Quarterly Journal of Engineering Geology and Hydrogeology, 43(2):141-155.

Delgado, J.; Vázquez, A.; Juncosa, R. & Barrientos, V. (2006). Geochemical assessment of the contaminant potential of granite fines produced during sawing and related processes associated to the dimension stone industry, Journal of Geochemical Exploration, 88(1-3):24-27.

IEC (2007). Safety of laser products - Part 1: Equipment classification and requirements - IEC 60825-1 Edition 2.0. International Electrotechnical Commission, p. 199.

Falcón, I. (2011). Los serrines de granito como barrera de impermeabilización para su uso en vertederos. PhD Dissertation, Department of Civil Engineering, University of A Coruña, A Coruña, 245 p.

Falcon-Suarez, I.; Rammlmair, D.; Juncosa-Rivera, R. & Delgado-Martin, J. (2014). Application of Rhizon SMS for the assessment of the hydrodynamic properties of unconsolidated fine grained materials. Engineering Geology, 172(0):69-76.

González, E.P.; Díaz-Pache, F.S.-T.; Mosquera, L.P. & Agudo, J.P. (2007). Bidimensional measurement of an underwater sediment surface using a 3D-Scanner. Optical and Laser Technology, 39(3):481-489.

Grossman, R.B. & Reinsch, T.G. (2002). The solid phase. Bulk density and linear extensibility. J.H. Dane & G. Clarke (eds), Methods of Soil Analysis, Part 4, SSSA, Madison, Wisconsin, p. 201-228.

Liu X.; Lu S.; Horton R. & Ren T. (2014). In Situ Monitoring of Soil Bulk Density with a Thermo-TDR Sensor. Soil Sciences Society of America Journal, 78(2):400-407.

Murray, E.J.; Rix, D.W. & Humphrey, R.D. (1992). Clay linings to landfill sites. Quarterly Journal of Engineering Geology and Hydrogeology, 25(4):371-376.

Navarro, V.; Barrientos, V.; Yustres, A. & Delgado J. (2008) Settlement of embankment fills constructed of granite fines. Computers and Geosciences, 34(8):978-992.

Nixon, M.; McCallum, B.; Fright, W. & Price, N. (1998). The effects of metals and interfering fields on electromagnetic trackers. Presence: Teleoperators Virtual Environments, 7(2):204-218.

Paajanen, M.; Katainen, J.; Pakarinen, O.H.; Foster, A.S. & Lahtinen J. (2006). Experimental humidity dependency of small particle adhesion on silica and titania. Journal of Colloid and Interface Science, 304(2):518-523.

Rossi, A. M.; Hirmas, D. R.; Graham, R. C. & Sternberg, P. D. (2008). Bulk density determination by automated three-dimensional laser scanning. Soil Science Society of America Journal, 72(6):1591-1593.

Rousseau, B.; Rivard, P.; Marache, A.; Ballivy, G. & Riss, J. (2012). Limitations of laser profilometry in measuring surface topography of polycrystalline rocks, International Journal of Rock Mechanics and Mining Sciences, 52(0):56-60.

Sander, T. & Gerke, H.H. (2007). Noncontact shrinkage curve determination for soil clods and aggregates by three-dimensional optical scanning. Soil Science Society of America Journal, 71(5):1448-1454.

Timm, L.C.; Pires, L.F.; Reichardt, K.; Roveratti, R.; Oliveira, J.C.M. & Bacchi, O.O.S. (2005). Soil bulk density evaluation by conventional and nuclear methods. Australian Journal of Soil Research, 43(1):97-103.

Vazquez, A.; Juncosa, R.; Barrientos, V.; Falcon, I.; Delgado, J. & Navarro, V. (2007). Hydrodynamic and reactive transport modeling of the behavior of compacted granite saw dust for landfill liners and covers. Proceedings of the 12th International Symposium on Water/Rock Interaction, Rotterdam, v. 1, pp. 653-659.

Yilmaz, H. M. (2007). The effect of interpolation methods in surface definition: an experimental study. Earth Surface Processes and Landforms, 32(9):1346-1361.

Zhang, T.; Zeng, Q.; Li, Y. & Xiang, Y. (2008). Study on relation between InSAR coherence and soil moisture. Proceedings of The International Archives of the Photogrammetry, Remote Sensing and Spatial Information Sciences, Beijing, v. 37 Part B7, pp. 131-134.